Evaluation and quantification of micro epithelial gaps in the colonic mucosa using immunofluorescence staining.
--Manuscript Draft--

Article Type:	Invited Methods Collection - Author Produced Video
Manuscript Number:	JoVE62204R1
Full Title:	Evaluation and quantification of micro epithelial gaps in the colonic mucosa using immunofluorescence staining.
Corresponding Author:	Porfirio Nava, Ph.D. MEXICO
Corresponding Author's Institution:	
Corresponding Author E-Mail:	pnava@cinvestav.mx
Order of Authors:	Felipe Castro-Martínez
	María Encarnación-García
	Aurora Candelario-Martinez
	Oscar Medina-Contreras
	Genaro Patiño-Lopez
	Michael Schnoor
	Porfirio Nava, Ph.D.
Additional Information:	
Question	Response
Please indicate whether this article will be Standard Access or Open Access.	Standard Access (US$1200)
Please specify the section of the submitted manuscript.	Biology
Please confirm that you have read and agree to the terms and conditions of the author license agreement that applies below:	I agree to the Author License Agreement
Please provide any comments to the journal here.	
Please indicate whether this article will be Standard Access or Open Access.	Standard Access ($1400)

1 **TITLE:**
2 **Evaluation and Quantification of Micro Epithelial Gaps in the Colonic Mucosa using**
3 **Immunofluorescence Staining**
4
5 **AUTHORS AND AFFILIATIONS:**
6 Felipe Castro-Martínez[1, *], María del Rocío Encarnación-García[1, *], Aurora Candelario-Martinez[1, *],
7 Oscar Medina-Contreras[3], Genaro Patiño-Lopez[4], Michael Schnoor[2] and Porfirio Nava[1]
8
9 *These authors contributed equally to this work.
10
11 [1]Departamento de Fisiología, Biofísica y Neurociencias del Centro de Investigación y de Estudios
12 Avanzados (CINVESTAV), IPN. México DF, México
13 [2]Departamento de Biomedicina Molecular del Centro de Investigación y de Estudios Avanzados
14 (CINVESTAV), IPN. México DF, México
15 [3]Unidad de Investigación Epidemiológica en Endocrinología, y Nutrición (UIEEN), Hospital Infantil
16 de México Federico Gomez, Mexico City, Mexico
17 [4]Laboratorio de Investigación en Inmunología y Proteómica, Hospital Infantil de México Federico
18 Gómez, México City, México
19
20 **Corresponding author:**
21 Porfirio Nava (pnava@cinvestav.mx).
22
23 **Co-Authors:**
24 Felipe Castro-Martínez (castro.qfb@gmail.com)
25 María del Rocío Encarnación-García (rocio.egar@gmail.com)
26 Aurora Candelario (aurorac@fisio.cinvestav.mx)
27 Michael Schnoor (mschnoor@cinvestav.mx)
28 Oscar Medina-Contreras (omedina@himfg.edu.mx)
29 Genaro Patiño-Lopez (gpatino@himfg.edu.mx)
30
34
35 **SUMMARY:**
36 Here, we describe a new method to visualize the specific location of where transcellular and
37 paracellular permeability is enhanced in the inflamed colonic mucosa. In this assay, we apply a
38 10 kDa fluorescent dye conjugated to a lysine fixable dextran to visualize high permeability
39 regions (HPR) in the colonic mucosa.
40
41 **ABSTRACT:**
42 Epithelial cells lining the intestinal mucosa create a physical barrier that separates the luminal
43 content from the interstitium. Epithelial barrier impairment has been associated with the
44 development of various pathologies such as inflammatory bowel diseases (IBD). In the inflamed

45 mucosa, superficial erosions or micro-erosions that corrupt epithelial monolayers correspond to
46 sites of high permeability. Several mechanisms have been implicated in the formation of micro-
47 erosions including cell shedding and apoptosis. These micro-erosions often represent
48 microscopic epithelial gaps randomly distributed in the colon. Visualization and quantification of
49 those epithelial gaps has emerged as an important tool to investigate intestinal epithelial barrier
50 function. Here, we describe a new method to visualize the specific location of where transcellular
51 and paracellular permeability is enhanced in the inflamed colonic mucosa. In this assay, we apply
52 a 10 kDa fluorescent dye conjugated to a lysine fixable dextran to visualize high permeability
53 regions (HPR) in the colonic mucosa. Additional use of cell death markers revealed that HPR
54 encompass apoptotic foci where epithelial extrusion/shedding occurs. The protocol described
55 here provides a simple but effective approach to visualize and quantify micro-erosions in the
56 intestine, which is a very useful tool in disease models, in which the intestinal epithelial barrier is
57 compromised.
58
59 **INTRODUCTION:**
60 The gastrointestinal (GI) mucosa creates a physical barrier that separates the extracellular
61 environment and the internal host milieu, and is involved in the absorption of nutrients, water
62 and electrolytes. The intestinal barrier encompasses a mucus layer constituted of glycoproteins,
63 a monolayer of epithelial cells, and the underlying lamina propria are immune and stromal cells
64 reside. Intestinal epithelial cells forming the physical barrier are linked together by different
65 protein complexes, which includes the adherens junction (AJ), the tight junction (TJ) and the
66 desmosomes (DMs). Impairment in the epithelial barrier function augments intestinal
67 permeability and allows the translocation of harmful substances and pathogens from the lumen
68 to the interstitium[1]. There is an increasing number of illnesses where the epithelial barrier is
69 compromised, such as the inflammatory bowel diseases (IBD) like Crohn's disease (CD), ulcerative
70 colitis (UC) and indeterminate colitis (IC). The incidence of IBD is increasing worldwide, with a
71 prevalence approaching 0.5% in the West. Although the causes of IBD are unclear, the excessive
72 immune/inflammatory response triggered in the gut wall directly contributes to the epithelial
73 barrier disruption by limiting the reestablishment of intestinal epithelial homeostasis[2,3,4]. In
74 addition, patients with long-standing colonic inflammation are at high risk of developing
75 colorectal cancer (CRC)[5]. Other pathologies associated with intestinal epithelial barrier disruption
76 are irritable bowel syndrome, obesity, celiac disease, non-celiac gluten sensitivity, and food
77 allergies[6]. For these reasons, there is an urgent need for the development of experimental
78 approaches that allow analysis of the integrity of the intestinal epithelial barrier in animal models
79 mimicking the pathogenesis occurring in humans.
80
81 Here, we evaluated the gastrointestinal passive paracellular and the transcellular permeability
82 associated to an inflammatory process in the colonic epithelium using a simple technique. To
83 investigate the transmural flow of macromolecules, we measured the passive diffusion of FITC-
84 dextran (4 kDa) and RITC-dextran (10 kDa) in colonic sacs *ex vivo*. Furthermore, by injecting a
85 fluorescent 10 kDa lysine-fixable dextran into the lumen of the intestine sacs, we specifically
86 identified the areas with high permeability in the inflamed mucosa. The use of apoptosis markers
87 and antibodies against AJ proteins allowed us to demonstrate that high permeability areas in the
88 inflamed mucosa correspond to specific regions where epithelial cells undergo apoptosis and cell-

89 cell junctions are disrupted. This new technique can be used to evaluate the integrity of the
90 epithelium in any model where the intestinal epithelial barrier is compromised.
91
92 **PROTOCOL:**
93
94 All procedures were reviewed and approved by the CINVESTAV Institutional Committee for Care
95 and Use of Laboratory Animals (CICUAL).
96
97 **1.   Preparation of materials and reagents**
98
99 1.1.   Pre-warm Hartmann's solution (130 mM NaCl, 28 mM lactate, 4 mM KCl, 1.5 mM $CaCl_2$)
100 to 37 °C while bubbling with 95% O_2/5% CO_2. Maintain physiological pH (7.4) for the solution.
101
102 1.2.   For analyzing the passive paracellular permeability, prepare a working solution by
103 dissolving 1 mg/mL of FITC-Dextran (4 kDa) and 1 mg/mL of RITC-Dextran (10 kDa) in pre-warmed
104 Hartmann´s solution.
105
106 1.3.   Prepare a 4 µg/mL solution of Alexa Fluor647 Fixable-Dextran (10 kDa) in Hartmann's
107 solution. Store working solutions in a 15 mL conical tube and protect from the light until use.
108
109 NOTE: 300 µL of working solution per colon will be necessary.
110
111 1.4.   Prepare a surgical suture by cutting two 5 cm sections for each large intestine. Loop the
112 sutures into an unclosed knot.
113
114 **2.   Dissection and preparation of the gastrointestinal trac**
115
116 2.1.   Withhold solid food for 6 hours before euthanizing the mice. Provide ad libitum drinking
117 water.
118
119 NOTE: If possible, place the mice on nutrient gel supplements (purified Water, Molasses,
120 Pumpkin, Corn Syrup, Sunflower Seeds, Wheat Protein, Vegetable Oil, Food Acid, Hydrocolloids,
121 Electrolytes, Corn Fiber, NIH-31M Mineral Mix, NIH-31M Vitamin Mix).
122
123 2.2.   Euthanize mice in a CO_2 chamber followed by cervical dislocation in accordance with
124 institutional ethics protocols.
125
126 2.3.   Sterilize the abdomen and thorax with 70% ethanol.
127
128 2.4.   Using a pair of scissors, make an incision in the middle of the abdomen and expose the
129 peritoneal cavity.
130
131 2.5.   For orientation purposes, separate and dissect the large intestine by cutting at the end of
132 the small intestine (end portion of the ileum) right before the cecum and then at the anal verge.

133 Use surgical forceps to gently remove the mesentery and place the colon in Hartmann's solution.
134

135 2.6. Importantly, in order to maintain consistency between animals, identify similar sections
136 and use to evaluate permeability. Using regions close to the cecum is highly recommendable.
137

138 2.7. Use an insulin syringe equipped with a blunted plastic cannula to gently flush the luminal
139 content present in the colon. If the stool is firm, carefully push with the help of blunt forceps.
140 After the feces have been removed, wash 3 times with 400 µL of Hartmann's solution.
141

142 2.8. Tie the proximal region (closest one to the cecum) and place a pre-tied suture-loop in the
143 distal region of the colon. With the help of a syringe equipped with a blunted plastic cannula fill
144 the intestinal sac with the solution containing the desire probe. Carefully remove the plastic
145 cannula and tie the loop in the distal region.
146

147 2.9. Place the intestinal sac in a 15 mL conical tube with 6 mL of Hartmann's solution and
148 incubate for 1 h to evaluate the passive paracellular flow of FITC/RITC-Dextran or 30 min to
149 analyze the flow of the Alexa Fluor Fixable-Dextran.
150

151 2.9.1. Maintain the conical tubes containing the intestinal sacs at 37 °C with 5% CO_2 and
152 protect from light.
153

154 2.10. To measure the passive permeability using FITC/RITC-Dextran. At 0 and 60 min, take a 100
155 µL sample from the conical tube and transfer to a 96 well plate. Add back 100 µL of fresh media
156 to replace the volume lost.
157

158 2.11. Measure samples and standards for FITC/RITC on a fluorescent plate reader (FITC
159 excitation/emission: 495 nm/519 nm; RITC excitation/emission: 570/595 nm).
160

161 2.12. To measure the passive permeability using Alexa Fluor 647 Fixable-Dextran, remove the
162 intestines, cut close to the surgical tie knot, and cut the intestine to expose the lumen to remove
163 the solution with the probe. Wash the lumen of the intestine 2 times with cold Hartmann's
164 solution.
165

166 2.13. Place the tissue in a tissue-mold previously filled with Optimal Cutting Temperature
167 compound (O.C.T.). Orient the tissue vertically or horizontally according to the side to be
168 sectioned. Store the samples at -80 °C.
169

170 **3. Immunofluorescent staining**
171

172 3.1. Fix frozen sections of 20 micrometers with 3.7% paraformaldehyde (PFA) for 20 min at
173 room temperature and then wash 3 times with cold phosphate buffered saline (PBS; 37 mM NaCl,
174 2.7 mM KCl, 10 mM Na_2HPO_4, and 1.8 mM KH_2PO_4).
175

176 NOTE: Vertical sections from intestines tend to come off if the washes are very strong.

177

178   3.2.   Permeabilize with 0.2% TX-100/PBS for 12 min at room temperature and then wash 3
179   times with cold PBS.

180

181   3.3.   Block with 0.2% BSA/PBS for 1 hour at room temperature.

182

183   3.4.   Dilute the primary antibody in blocking solution and incubate for 1 h at room
184   temperature. Wash 3 times with cold PBS.

185

186   3.5.   Incubate for 1 h with secondary antibodies in blocking solution. Wash 3 times with cold
187   PBS.

188

189   3.6.   Apply mounting medium to the cuts and seal with a coverslip. The slides can be stored for
190   up to 3 months at -20 ° C.

191

192 **REPRESENTATIVE RESULTS:**
193 In the inflamed mucosa, superficial erosions or microerosions compromise the integrity of the
194 epithelial cell monolayer and represent sites of high permeability[7,8]. To assess such possibilities,
195 we analyzed the passive permeability in the inflamed colonic mucosa in a dextran sodium sulfate
196 colitis murine model. In brief, for 5 days, C57BL/6J mice received 2.5% DSS (w/v, 40-50 kDa)
197 dissolved in drinking water. This model is characterized by inducing epithelial cell damage and
198 epithelial barrier dysfunction in the large intestine, which in turns allows the entrance of luminal
199 antigens into the lamina propria. Such a process results in stimulation of the immune system,
200 leading to the secretion of proinflammatory cytokines and chemokines that further enhance the
201 epithelial damage[9]. As shown in **Figure 1A**, the mice exposed to DSS exhibited a ~12% body
202 weight loss after 5 days of treatment. Fecal blood and diarrhea were also detected in all DSS-
203 treated mice. Additionally, colitic mice displayed a reduction in colon length that was statistically
204 significant (**Figure 1B**). Thus, the disease activity index (DAI) encompassing animal weight loss,
205 stool consistency, diarrhea, occult blood, and gross rectal bleeding increased after 5 days of DSS
206 treatment (**Figure 1C**). Histopathological analysis revealed the presence of epithelial erosions,
207 ulcerations, immune infiltrate and edema in the colonic mucosa of colitic mice (**Figure 2**).

208

209 Epithelial barrier disruption, including intestinal epithelial cell apoptosis and dysfunctional
210 intercellular junctions, have been accounted for the increase in passive permeability in the
211 inflamed mucosa[10, 11]. Therefore, we indirectly measured the permeability in the colonic mucosa
212 by monitoring the passive flow of fluorescently labelled probes (FITC and RITC-dextran). As shown
213 in **Figure 3A**, the inflammatory process induced after DSS administration augmented transmural
214 permeability, as shown by the increase in the passive flow of FITC-dextran (4 kDa) and RITC-
215 dextran (10 kDa). In addition, as shown in **Figure 3B**, Western blot analysis confirmed the increase
216 of apoptosis in the colonic mucosa of DSS-treated mice as shown by the presence of active
217 caspase 3 (Acasp-3). Thus, the data strongly suggest that during inflammation the apoptotic
218 process triggered in the inflamed mucosa contribute to the disruption of the epithelial barrier
219 function.

220

221 Next, we assessed the localization of the areas with high permeability in the inflamed mucosa by
222 analyzing the flow of a fluorescent fixable lysine dextran of 10 kDa. We used a 10 kDa molecule
223 to restrict the flow only to highly permeable regions with high pore size. In control mice, the
224 fixable dextran was retained at the apical surface of the colonic crypts (white arrows) and was
225 delimited by the tight bundle of actin filaments at the brush border microvillus (**Figure 4A**).
226 However, in colitic mice, the fixable dextran permeated into the cytosol of colonic epithelial cells
227 demonstrating that inflammation induces active transcellular flow (asterisks). Upon further
228 analysis we observed the presence of fixable dextran in the interstitium in colitic mice (arrows)
229 but not in control animals, indicating a net flow from the luminal to the interstitial side (**Figure**
230 **4B**). In the leaky area, the cytosolic fixable dextran was clearly incorporated in epithelial cells
231 grouped in microregions at the luminal side and those cells were positive for the apoptotic
232 marker Acasp-3 (**Figure 4C**). Importantly, also at the surface in the areas of high permeability
233 where the epithelial cells undergo apoptosis (apoptotic foci) we noticed an aberrant distribution
234 for E-cadherin (**Figure 4C, Arrows**) and effect not observed in control tissue. Additionally, the
235 results showed that the fixable dextran was internalized in anoikis cells present at the lumen, and
236 some of those cells displayed a faint cytosolic staining for E-cadherin (arrowhead) (**Figure 4D**).
237 Contrary to E-cadherin the intestinal epithelial cells enriched with cytosolic fixable dextran shown
238 a clear staining for ZO-1 at the TJ (**Figure 4E**), no staining for ZO-1 was detected in detached cell
239 (Data not shown). Thus, in conclusion we demonstrated that fixable dextran is a good tool to
240 identify sites of high permeability in the gut and is internalized in apoptotic and anoikis cells.
241
242 **FIGURE AND TABLE LEGENDS:**
243
244 **Figure 1. Induction of acute colitis using DSS.** (**A**) Daily changes in body weight of C57BL/6J mice
245 treated with 2.5% DSS for 5 days. Body weight is expressed as a percentage of the body weight
246 at day 0. (**B**) Macroscopic changes observed in the colons of mice treated with DSS for 5 days.
247 *Upper panel*. Representative image of colons harvested from control and colitic mice. *Lower*
248 *panel*. Shortening of the colon length was observed in DSS-treated mice. (**C**) Clinical score
249 (Disease Activity Index; DAI) over 5 days following water (controls; n 5) or 2.5% dextran sodium
250 sulphate (DSS) oral treatment. The DAI encompassing body weight loss, consistency stool and
251 blood in feces was increased in colitic mice. Data are presented as the means ± SEM (n=5). P
252 values were calculated using a two-way ANOVA with Sidak´s post hoc test (**A**) and Student's t test (**B**,
253 **C**). **p < 0.01; ***p < 0.001.
254
255 **Figure 2. Microscopic changes in the colonic mucosa of healthy and DSS-treated mice**. At the
256 end of the experiment, the animals were euthanized, and the tissue specimens were fixed,
257 embedded in paraffin, sectioned and stained with hematoxylin and eosin (H&E). Infiltration of
258 inflammatory cells (arrow), ulcerations (arrowhead) and loss of cryptal architecture (erosion, e)
259 were observed in the colon of DSS-treated mice.
260
261 **Figure 3. Passive paracellular transport of Fluorescent labeled Dextran is enhanced during**
262 **colitis.** (**A**) Analysis of passive paracellular transport of fluorescent labeled dextran in intestinal
263 sacs of healthy and colitic mice. Intestinal sacs were prepared from colons harvested from age
264 matched C57BL/6J mice treated with water or 2.5% DSS for 5 days. Sacs were loaded with a

solution containing 1 mg/ml of FITC-dextran-4 kDa (MW 4,400 Da) and 1 mg/ml of RITC-dextran-10 kDa (MW 10,000 Da). Passive paracellular flux of the fluorescent probes was measured after 60 min. Paracellular permeability is augmented after colitis induction. (**B**) Evaluation of Active Caspase-3 (Acasp-3) in the colonic mucosa of DSS-treated mice. Whole cell lysates were prepared from colonic samples harvested from age matched C57BL/6J mice treated with water or 2.5% DSS for 5 days. 30 µg of protein were loaded and separated in 12% SDS-polyacrylamide gels, transferred to a nitrocellulose membrane and western blotted for Acasp-3. GAPDH was used as loading control. The presence of active Caspase-3 is augmented after colitis induction. n = 5. Data are presented as the means ± SEM (n=5). P values were calculated using a two-way ANOVA with Sidak´s post hoc test (A) and Mann- Whitney test (B). *p < 0.05 ***p < 0.001.

Figure 4. Identification of permeability sites in the colonic mucosa of healthy and DSS-treated mice. Intestinal sacs were prepared from colons harvested from age matched C57BL/6J mice treated with water or 2.5% DSS for 6 days. Sacs were loaded with a solution containing 4 µg/mL of fixable Alexa Fluor 647 dextran, 10 kDa. Passive paracellular flux of the fluorescent probe was stopped after 30 min. The colonic sacs were fixed, embedded in OCT, sectioned and stained for immunofluorescence. (**A**) In control conditions, the fixable dextran (red) was detected in close apposition with (arrows) the apical actin ring (green) limiting the apical surface of the colonocytes facing the luminal side. After DSS treatment, the continuity of the apical actin ring was disrupted (asterisk). The fixable dextran permeated into the cytosol of surface epithelial cells. (**B**) Analysis of fixable dextran and E-cadherin at sites of high permeability. In control conditions the fixable dextran was retained at the luminal side. In the colitic mucosa, fixable dextran was detected at the cytosol of epithelial cells lining the crypt surface and in several regions of the interstitium (Arrows). Epithelial cells that incorporated fixable dextran were located at the crypt surface and showed an aberrant distribution of E-cadherin. Dash line delimits the crypt. n = 5. (**C**) Analysis of Active caspase-3 and E-cadherin at the sites of high permeability identified with the fixable dextran in the colonic mucosa of colitic mice. Active caspase-3 (green) was enriched at the sites of high permeability. Arrows mark epithelial cells with aberrant staining for E-cadherin that were present at the crypt surface. n = 5. (**D**) Analysis of fixable dextran and E-cadherin. In control conditions the fixable dextran was retained at the luminal side. In the colitic mucosa, fixable dextran was detected at the cytosol of detached epithelial cells located at the intestinal lumen (Arrows). Epithelial cells marked with fixable dextran showed a clear presence of cytosolic E-cadherin. n = 5. (E) Analysis of fixable dextran and ZO-1. In control conditions the fixable dextran was retained at the luminal side above the TJ (marked by ZO-1). In the colitic mucosa, fixable dextran was detected at the cytosol of detached epithelial cells and in epithelial cells at the crypt surface (asterisks). ZO-1 localized at the TJ in control and colitic conditions (Arrows). n = 5.

DISCUSSION:
Epithelial homeostasis resulting from balancing cell proliferation and epithelial apoptosis maintains a proper and functional intestinal barrier. Many clinical disorders, such as IBD, are accompanied or characterized by alterations in intestinal permeability, inflammation of the mucosa and disruption of the epithelial homeostasis[1]. The interplay between those processes is still highly controversial. Therefore, the development of new research approaches to properly investigate those processes is an important subject in the field. There are several published

309   protocols available for indirectly studying the intestinal permeability during inflammation, such
310   as the measurement of transepithelial electrical resistance in epithelial monolayers and
311   quantification of hydrophobic fluorophore-labeled probes in intestinal organoids, mouse
312   intestines and intestinal sacs[10–13]. Despite demonstrating that the uptake of a substance
313   increases or decreases in the intestinal mucosa, those methods fall short in analyzing other
314   important events that directly contribute to the changes in the permeability. For example, by
315   failing to identify the specific areas where the integrity of the epithelium is compromised, those
316   studies limit the understanding of the transport mechanisms or the biological functions
317   responsible for affecting the intestinal permeability. Furthermore, given that the intestinal
318   permeability may vary greatly by region, those studies could generate errors such as false positive
319   results. Therefore, complementing those studies with non-quantitative site-specific assessments
320   such as the one described here will allow to determine the exact region where the flow of
321   substances occurs in the damaged epithelium. This new permeability assay not only allows a
322   better understanding of the regional mucosal integrity in digestive diseases but also permits the
323   study of the disrupted mechanisms contributing to such process.

325   The new technique described is a combination of two previously described techniques, the
326   preparation of intestinal sacs to assess mucosal barrier function *ex vivo*[12] and the use of fixable
327   fluorescent tracers to analyze brain vascular permeability[13]. By using this technique, we observed
328   that epithelial barrier impairment after IEC damage enhances the general flow of luminal
329   antigens to the interstitial compartment. The use of a 10 kDa fixable dextran was chosen to
330   specifically analyze the localization of highly permeable areas with a big pore size in the colitic
331   mucosa. Therefore, the high permeability sites in the inflamed mucosa that were detected here
332   encompass apoptotic foci where surface colonocytes undergo apoptosis or extrusion, a process
333   known as anoikis. However, the use of probes of different sizes could be a useful tool to
334   discriminate where the paracellular and transcellular flow is affected in the gut. Of note, cells
335   undergoing apoptosis/anoikis always incorporated 10 kDa fixable dextran, making the technique
336   useful to identify the areas where the plasma cell membranes of the epithelial cells are
337   compromised. During anoikis, several cell-cell junction molecules are lost or redistributed, and
338   the technique could also be helpful to identify those proteins. In fact, here we observed that E-
339   cadherin is lost from the lateral plasma membrane or internalized in IEC labeled with fixable
340   dextran. Thus, the results presented here demonstrate that the augment in the intestinal
341   permeability during inflammation is affected by the disruption in the epithelial barrier continuity
342   caused by IEC death (apoptosis/anoikis) and not only by disturbance in the function of the tight
343   junctions[14].

345   To our knowledge, a similar protocol employs confocal laser endomicroscopy *in vivo* to evaluate
346   the presence of micro-erosions and epithelial damage in the intestine in real time. Such a
347   technique identifies extruding cells in the inflamed and non-inflamed mucosa of the intestine.
348   However, in the absence of specific markers to evaluate the mechanisms, the cell type and even
349   the machinery involved in the disruption of the epithelial integrity this protocol is very limited[8].
350   In addition, using this technique we cannot measure the degree of epithelial perturbation, the
351   integrity of the mucous gel layer, or the presence of subtle changes that may not be apparent.
352   Also, the presence of regional changes in barrier function could be lost. Therefore, our protocol

353 appears as a stronger option to investigate the epithelial barrier permeability in the intestinal
354 mucosa. However, it must be taken in account that our method uses fixed tissue and therefore
355 the observations correspond to postmortem or biopsied tissue.
356
357 In conclusion, the protocol described here provides a simple but effective approach to visualize
358 and quantify microerosions and epithelial cell death (apoptosis/anoikis) in the intestine, which is
359 a very useful tool in disease models in which the intestinal epithelial barrier is compromised.
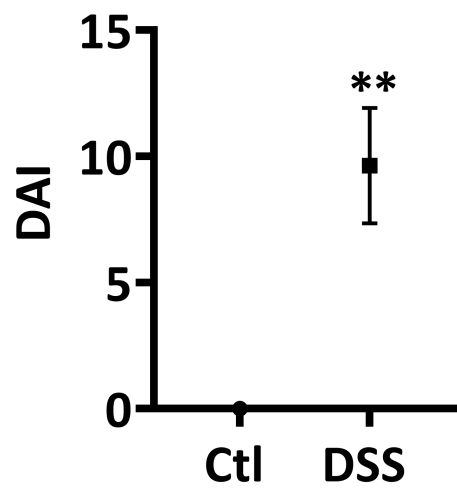360

367

368 **DISCLOSURES:**
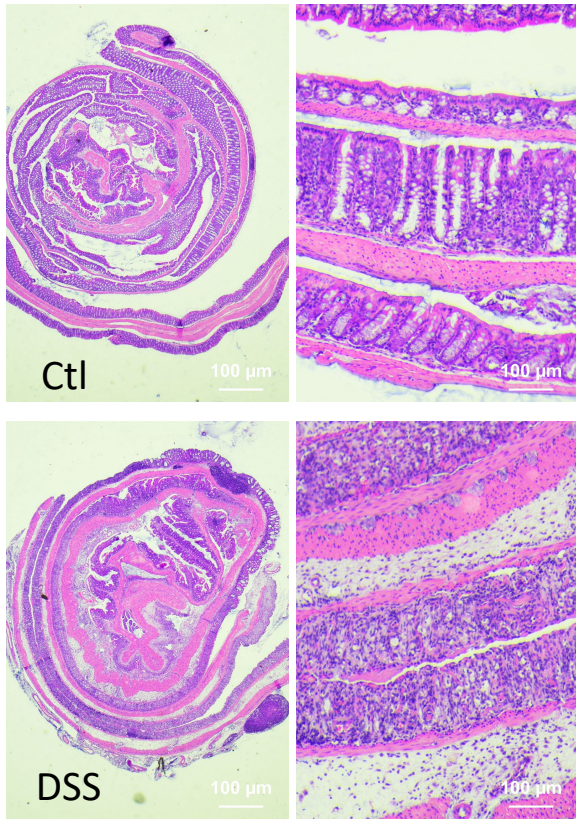369 The authors have nothing to disclose.
370
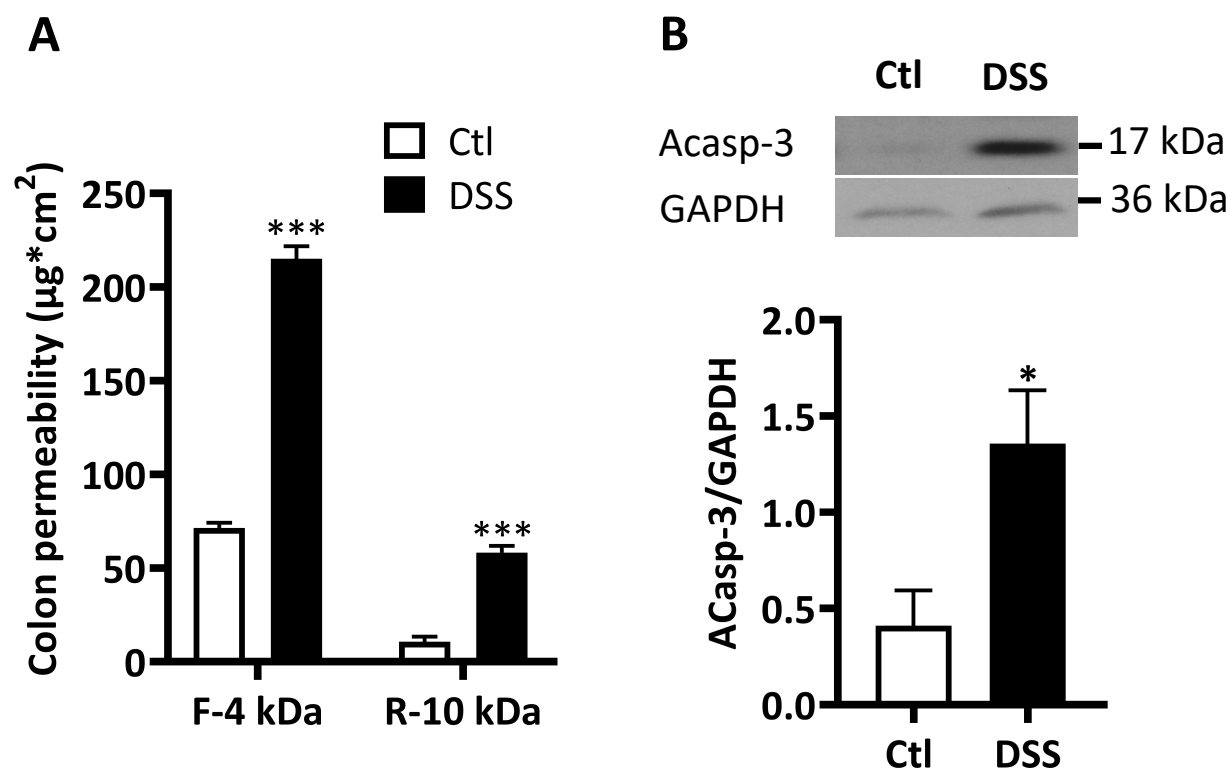
371 **REFERENCES:**
372 1.   König, J. *et al.* Human Intestinal Barrier Function in Health and Disease. *Clinical and*
373 *Translational Gastroenterology*. **7** (10), e196, doi: 10.1038/ctg.2016.54 (2016).
374 2.   Gassler, N. *et al.* Inflammatory bowel disease is associated with changes of enterocytic
375 junctions. *American Journal of Physiology-Gastrointestinal and Liver Physiology*. **281** (1), G216–
376 G228, doi: 10.1152/ajpgi.2001.281.1.G216 (2001).
377 3.   Negroni, A., Cucchiara, S., Stronati, L. Apoptosis, Necrosis, and Necroptosis in the Gut and
378 Intestinal Homeostasis. *Mediators of Inflammation*. **2015**, 250762, doi: 10.1155/2015/250762
379 (2015).
380 4.   Nava, P. *et al.* Interferon-γ regulates intestinal epithelial homeostasis through converging
381 β-catenin signaling pathways. *Immunity*. **32** (3), 392–402, doi: 10.1016/j.immuni.2010.03.001
382 (2010).
383 5.   Choi, C.-H.R., Bakir, I.A., Hart, A.L., Graham, T.A. Clonal evolution of colorectal cancer in
384 IBD. *Nature Reviews Gastroenterology & Hepatology*. **14** (4), 218–229, doi:
385 10.1038/nrgastro.2017.1 (2017).
386 6.   González-González, M., Díaz-Zepeda, C., Eyzaguirre-Velásquez, J., González-Arancibia, C.,
387 Bravo, J.A., Julio-Pieper, M. Investigating Gut Permeability in Animal Models of Disease. *Frontiers*
388 *in Physiology*. **9**, doi: 10.3389/fphys.2018.01962 (2019).
389 7.   Poulsen, S.S., Pedersen, N.T., Jarnum, S. "Microerosions" in rectal biopsies in Crohn's
390 disease. *Scandinavian Journal of Gastroenterology*. **19** (5), 607–612 (1984).
391 8.   Neumann, H. *et al.* Assessment of Crohn's disease activity by confocal laser
392 endomicroscopy. *Inflammatory Bowel Diseases*. **18** (12), 2261–2269, doi: 10.1002/ibd.22907
393 (2012).
394 9.   Laroui, H. *et al.* Dextran Sodium Sulfate (DSS) Induces Colitis in Mice by Forming Nano-
395 Lipocomplexes with Medium-Chain-Length Fatty Acids in the Colon. *PLoS ONE*. **7** (3), doi:
396 10.1371/journal.pone.0032084 (2012).

397 10.   John, L.J., Fromm, M., Schulzke, J.-D. Epithelial barriers in intestinal inflammation.
398 *Antioxidants & Redox Signaling*. **15** (5), 1255–1270, doi: 10.1089/ars.2011.3892 (2011).
399 11.   Su, L. *et al.* TNFR2 activates MLCK-dependent tight junction dysregulation to cause
400 apoptosis-mediated barrier loss and experimental colitis. *Gastroenterology*. **145** (2), 407–415,
401 doi: 10.1053/j.gastro.2013.04.011 (2013).
402 12.   Mateer, S.W., Cardona, J., Marks, E., Goggin, B.J., Hua, S., Keely, S. Ex Vivo Intestinal Sacs
403 to Assess Mucosal Permeability in Models of Gastrointestinal Disease. *Journal of Visualized
404 Experiments: JoVE*. (108), e53250, doi: 10.3791/53250 (2016).
405 13.   Devraj, K., Guérit, S., Macas, J., Reiss, Y. An In Vivo Blood-brain Barrier Permeability Assay
406 in Mice Using Fluorescently Labeled Tracers. *Journal of Visualized Experiments: JoVE*. (132), doi:
407 10.3791/57038 (2018).
408 14.   Stamatovic, S.M., Johnson, A.M., Sladojevic, N., Keep, R.F., Andjelkovic, A.V. Endocytosis
409 of tight junction proteins and the regulation of degradation and recycling. *Annals of the New York
410 Academy of Sciences*. **1397** (1), 54–65, doi: 10.1111/nyas.13346 (2017).
411 15.   Srinivasan, B. *et al.* TEER Measurement Techniques for In Vitro Barrier Model Systems.
412 *Journal of Laboratory Automation*. **20** (2), 107–126, doi: 10.1177/2211068214561025 (2015).
413 16.   Pearce, S.C. *et al.* Marked differences in tight junction composition and macromolecular
414 permeability among different intestinal cell types. *BMC Biology*. **16** (1), 19, doi: 10.1186/s12915-
415 018-0481-z (2018).
416 17.   Laukoetter, M.G. *et al.* JAM-A regulates permeability and inflammation in the intestine in
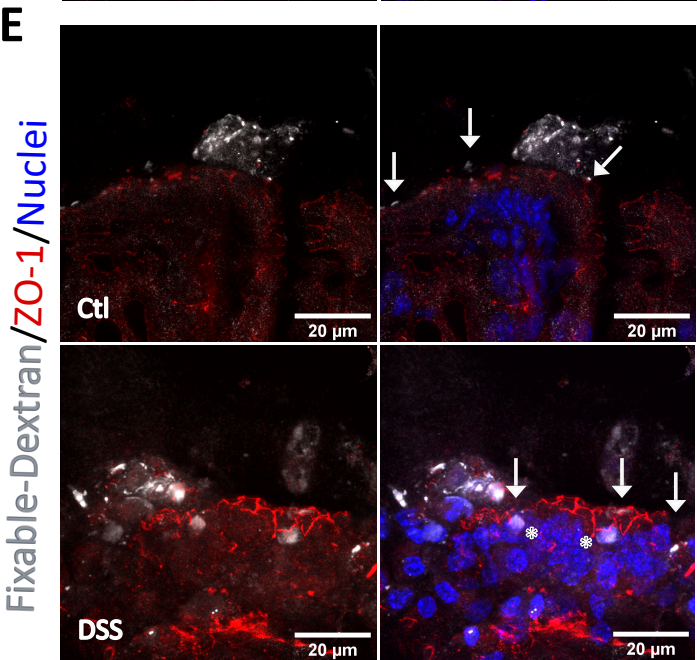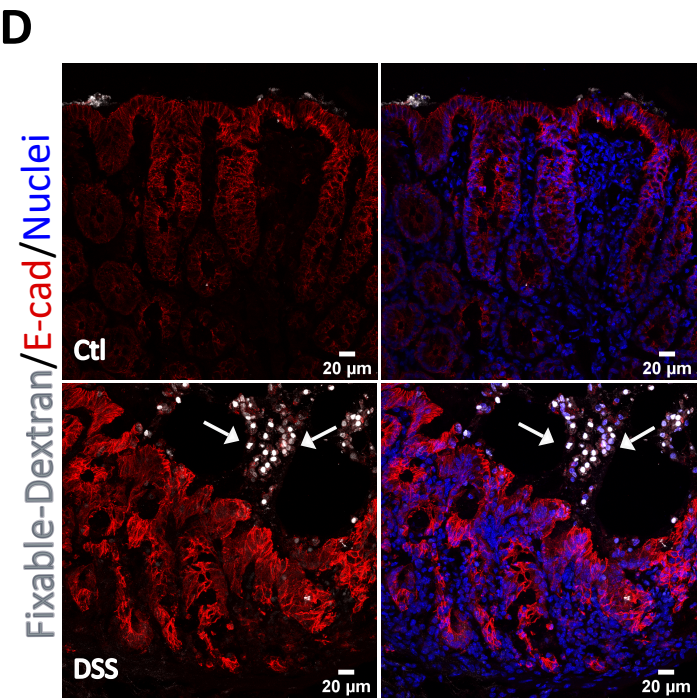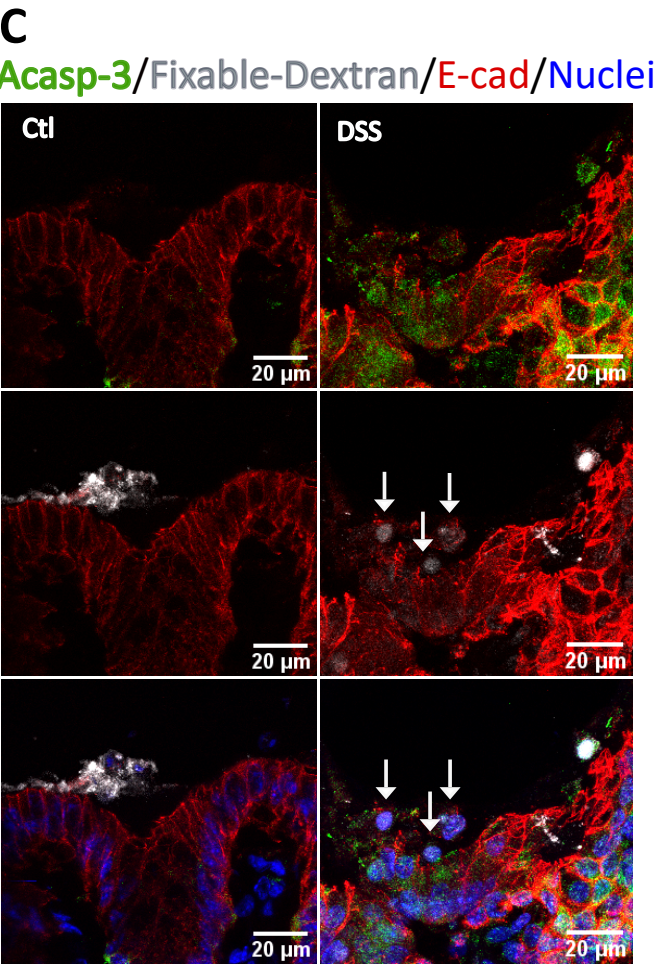417 vivo. *The Journal of Experimental Medicine*. **204** (13), 3067–3076, doi: 10.1084/jem.20071416
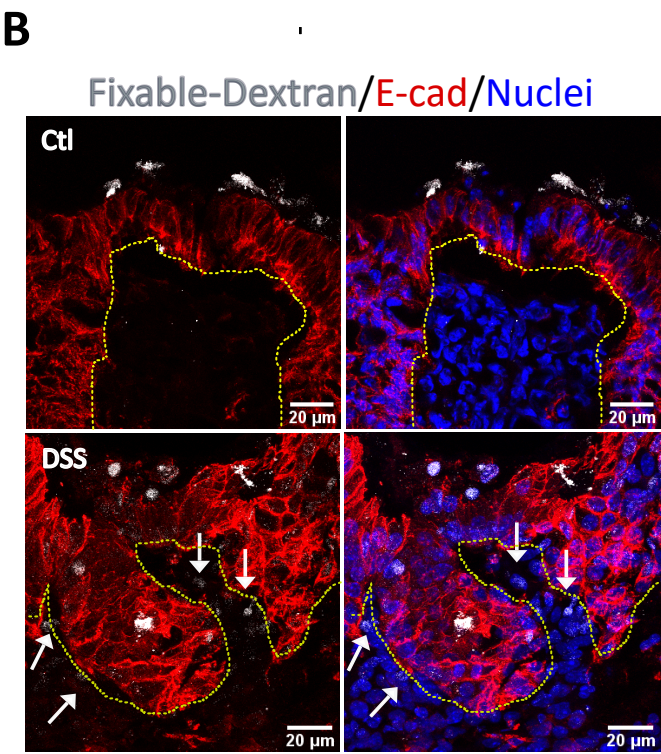418 (2007).
419

Figure 1

A

B

C

Figure 2

Click here to access/download;Figure;Figure 2.pdf

A

Figure 3

A

B

Figure 4
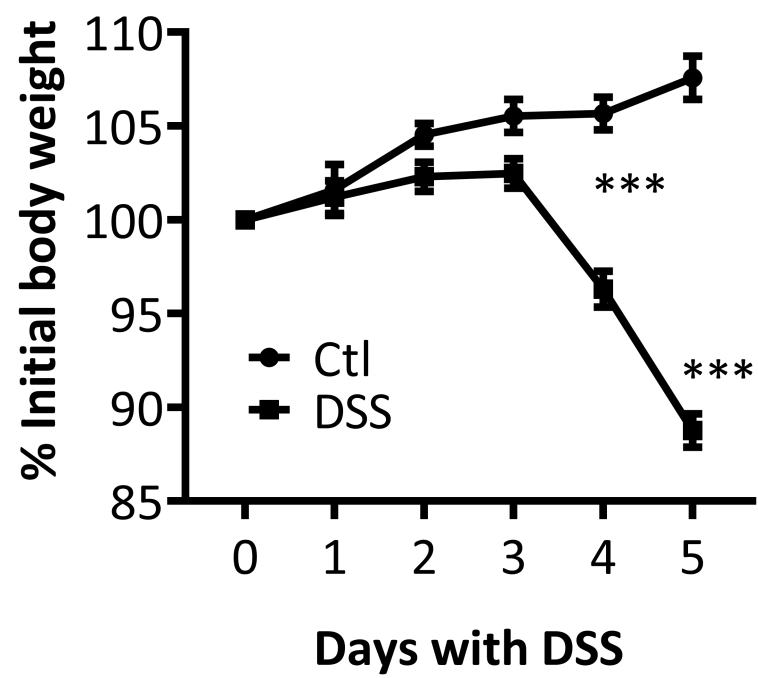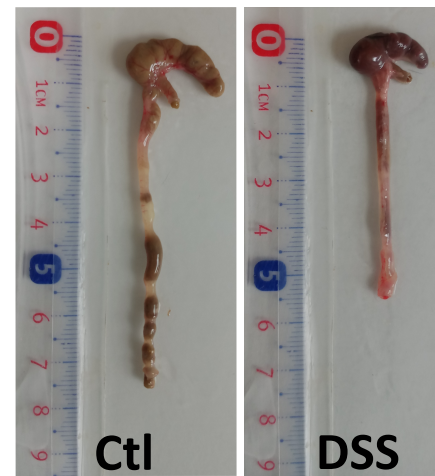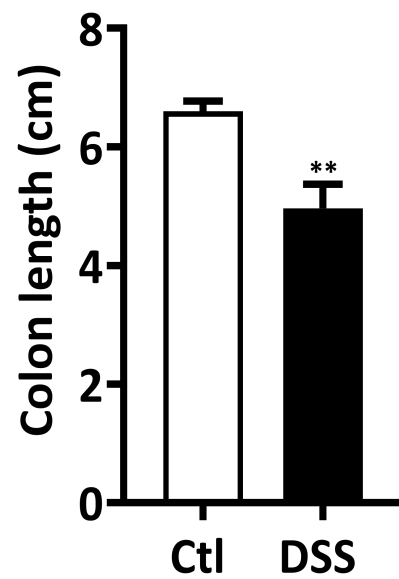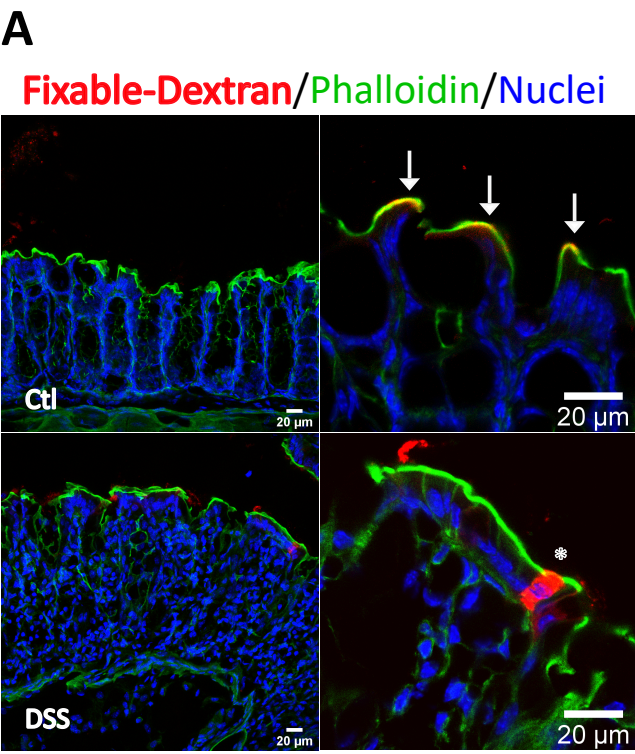
Name	Company	Catalog #	Description
Active Caspase-3 antibody (1:1000)	Cell signaling	9664	Cleaved caspase-3 (Asp175)(5AE1) Rabbit mAb
Alexa Fluor 488 anti rabbit (1:1000)	Invitrogen	A21206	
Alexa Fluor 594 anti rat (1:1000)	Invitrogen	A21209	
Confocal microscope (Leica TCS SP8x)	Leica		HyD detectors and White Light Laser
E-Cadherin antibody (1:750)	Sigma	MABT26	Rat monoclonal Delma-1 antibody
Ethanol 70%	Generic		
Fixable-Dextran	Invitrogen	D22914	Dextran, Alexa Fluor, 10,000 MW, anionic, fixable
FITC Dextran	Sigma	46944	Fluorescein isothiocyanate–dextran M. Wt. 4 kDa
Hartmann's Solution	PiSA	HT PiSA	
Incubator (AutoFlow NU-8500)	Nuaire		
Microplate reader (Tecan Infinite 200 PRO)	Tecan		
Nunc F96 MicroWell Black and White Polystyrene Plate	ThermoFisher Scientific		
Paraformaldehyde	Sigma	P6148	
Phalloidin (1:1000)	Invitrogen	A12380	Alexa Fluor 568 Phalloidin
RITC Dextran	Sigma	R8881-100MG	Rhodamine B Isothiocyanate-Dextran. M. Wt. 10 kDa
Secondary antibodies (1:10000)	Jackson ImmunoResearch Laboratories		HRP-conjugated secondary antibodies
Suture threads	Generic		Braided silk and braided polyester surgical sutures are prefered.
ZO-1 (1:1000)	Invitrogen	40-2200	Rb anti-ZO-1

Manuscript # JoVE62204

April 5, 2021

Dr. Nam Nguyen

Manager of Review

JoVE

RE: Manuscript No. JoVE62204

Dear Dr. Nguyen:

Please find enclosed our revised manuscript entitled "Evaluation and quantification of micro epithelial gaps in the colonic mucosa using immunofluorescence staining." and a rebuttal letter addressing in a point-by-point fashion reviewer's concern. We thank the reviewers for their helpful comments that have improved our manuscript. The corresponding changes in the revised manuscript have been highlighted in red color. We hope our manuscript is now suitable for publication in JoVE.

Thank you in advance for your consideration.

Sincerely,

Dr. Porfirio Nava

Cinvestav, IPN

Editorial and production comments:

Changes to be made by the Author(s):

1. Please take this opportunity to thoroughly proofread the manuscript to ensure that there are no spelling or grammar issues.

2. JoVE cannot publish manuscripts containing commercial language. This includes trademark symbols (™), registered symbols (®), and company names before an instrument or reagent. Please remove all commercial language from your manuscript and use generic terms instead. All commercial products should be sufficiently referenced in the Table of Materials. **As requested, proper commercial language was incorporated.**

3. Please specify what is Hartmann's solution. What is its composition? **The information was incorporated.**

4. What are the concentrations of the antibodies used? **The information was incorporated**.

Please upload a high-resolution video here so that we can review the video as well: https://www.dropbox.com/request/IZZspGb9ecJqhVIZue5p?oref=e

Reviewers' comments:
Reviewer #1:
Manuscript Summary:
The manuscript focuses on the evaluation and quantification of micro epithelial gaps in the colon mucosa by immunofluorescence staining. The authors described a detailed protocol of preparing intestinal sacs and immunofluorescent staining with fixable fluorescent traces. With the described protocol, a clear and typical image could be captured. The description is clear and easy to read, provides a new technique to assess the epithelial barrier impairment. Therefore, the present study is suitable for publication.

Minor Concerns:
1:Figure1B: the images of colon tissue should also be labeled.

Answer: As requested proper labels were incorporated in figure 1B.
2:Figure4B: Green Acasp-3 is followed by a red "/", which may mislead the reader.

Answer: As requested all panels in figure 4 were properly labeled.

3:Figure3B: The western blotting images should also be analyzed, and bar charts should be added.

Answer: As requested densitometric analysis was performed and incorporated in figure 3B.

Reviewer #2:

Manuscript Summary:

This manuscript describes a method for the detection of microerosions and breaks in the intestinal epithelium, such as that which occurs in inflammatory diseases of the gut. In their studies, they use the DSS model of murine colitis, a standard and well accepted model. The authors use FITC- and RITC-dextran to measure permeability in an ex vivo colonic sac preparation. A fixable dextran tagged with Alexa Fluor 647 is used to mark areas of epithelial permeability, at sites of epithelial apoptosis for example. The manuscript would be strengthened by addressing the following comments.

Major Concerns:

Line 169-170. The authors say that "colitic mice displayed a reduction in colon length that was statistically significant". However, no indication of statistical difference is shown in Figure 1B.

Answer: We apologize for our mistake proper labels for statistical analysis were incorporated in figure 1B.

Line 274-276. The authors state that they "observed that epithelial barrier impairment after IEC damage enhances the transcellular and paracellular flow of luminal antigens into the intestinal compartment". The data do not support this statement. There is movement of marker molecules into apparently damaged/apoptotic IEC, but no evidence of transcellular movement. Evidence of paracellular movement is not convincing.

Answer: We agree with the reviewer and the statement is now modified and now reads. "By using this new technique, we observed that epithelial barrier impairment after IEC damage enhances the general flow of luminal antigens to the interstitial compartment. The use of a 10kDa fixable dextran was chosen to specifically analyze the localization of highly permeable areas in the colitic mucosa. However, the use of probes with different sizes could be a useful tool to determine where the paracellular and transcellular flow is affected. ".

Line 278-279. The authors say that "several cell-cell junction molecules were lost or redistributed". Are they referring to this study? If so, the statement is not supported by evidence since they only assessed one junctional protein. If they are referring to another paper, then a reference is necessary.

Answer: We agree with the reviewer an image showing changes in ZO-1 was now incorporated.

Line 280-281. The authors state that "E-cadherin…was redistributed from the lateral plasma membrane to the cytosol…". The evidence to support this statement is not convincing. In Fig 4B, there is even distribution of red throughout the cytoplasm of all the cells. It looks more like non-specific staining. How do we know if this is an inflammation-mediated event when there is no control with which to compare?

Answer: We agree with the reviewer a better image depicting our findings was already incorporated and the statement modified accordingly "this molecule was lost from the lateral plasma membrane in IEC labeled with fixable dextran".

Figure 2. This micrograph shows extensive damage to the colonic mucosa, with virtually no epithelium left. Is this representative of the state of the colon used in subsequent experiments? It does not seem to match the micrographs in Figure 4.

Answer: Microerosions in the colitic mucosa are randomly observed. A more representative image of the colonic mucosa obtained after DSS-treatment (low magnification) has been now incorporated.

Figure 4. It is not clear that the micrographs in this figure support the conclusions drawn by the authors. In Fig 4A, the colocalization of fixable dextran with phalloidin indicates permeability of the epithelial cell membrane, not epithelial permeability. A better demonstration of subepithelial localization of the fixable dextran is needed before saying that there is increased epithelial permeability. Overall it seems that the authors have illustrated fixable dextran is a marker of apoptotic/dying cells. In the bottom-right panel, it appears that an extruding cell is loaded with the fixable dextran, as is a cell within the epithelium. There is no evidence that this marker is showing changes in permeability. Indeed, in Fig 4B, top-right and bottom-left panels, staining for fixable dextran colocalizes almost exclusively with activated caspase 3 immunoreactivity. There is no evidence of fixable dextran anywhere else in the image.

Answer: Thanks for your criticism. Figure 4 has been replaced with several images that better depict our findings. In addition, a new description of the figure has been incorporated.

Minor Concerns:
Line 95. "reactive" should be "reagents". We apologize for the mistake.
Line 96. Define the composition of Hartmann's solution. The information was incorporated.
Line 109. Describe the nutrient gel supplements or provide a reference. The information was incorporated.
Line 117-118. The authors suggest using regions close to the cecum. Why? **Answer: Regions close to the cecum are used only as orientation purposes and to maintain the uniformity of the samples.**

Line 133-134. The authors state that the excitation/emission wavelengths of RITC are 495/519 nm. In fact, they are 570/595 nm. We apologize for the mistake.
Line 139. Define O.C.T. The information was incorporated.
Line 144. Define PFA. The information was incorporated.
Line 145. Define the composition of PBS. The information was incorporated.

Reviewer #3:
Manuscript Summary:
Intestinal epithelial barrier impairment is a pathological hallmark of inflammatory bowel diseases. In inflamed mucosa superficial epithelial micro-erosions correspond to sites of high intestinal permeability. Here the authors describe a new method to visualize the specific location of where

permeability is enhanced in inflamed colonic mucosa. Some minor concerns are listed below.

Minor Concerns:
It is unclear what samples have been run in the western blot in Fig. 3. A GAPDH blot with individual bands viable would also improve this figure.

Answer: Proper labeling in Fig 3A and a new GAPDH blot was incorporated as requested.

It would be useful to provide additional images for Fig.4A to better highlight how the dextran permeates in between the epithelial cells in colitic mice. Is there a way of quantifying how many of these high permeability sites were identified?

Answer: We understand the reviewers concerns. A better image depicting our findings has been incorporated. Quantification of permeability sites could be done using the method currently described here however it is out of the scope of the current manuscript.